The Journal of Immunology

The Optimal Antigen Response of Chimeric Antigen Receptors Harboring the CD3 ζ Transmembrane Domain Is Dependent upon Incorporation of the Receptor into the Endogenous TCR/CD3 Complex

John S. Bridgeman, Robert E. Hawkins, Steve Bagley, Morgan Blaylock, Mark Holland and David E. Gilham

J Immunol 2010; 184:6938-6949; Prepublished online 17 May 2010;
doi: 10.4049/jimmunol.0901766
http://www.jimmunol.org/content/184/12/6938

The Journal of Immunology is published twice each month by
The American Association of Immunologists, Inc.,
1451 Rockville Pike, Suite 650, Rockville, MD 20852

Print ISSN: 0022-1767 Online ISSN: 1550-6606.

The Optimal Antigen Response of Chimeric Antigen Receptors Harboring the CD3ζ Transmembrane Domain Is Dependent upon Incorporation of the Receptor into the Endogenous TCR/CD3 Complex

John S. Bridgeman,* Robert E. Hawkins,* Steve Bagley,† Morgan Blaylock,‡ Mark Holland,§ and David E. Gilham*

Chimeric Ag receptors (CARs) expressed in T cells permit the redirected lysis of tumor cells in an MHC-unrestricted manner. In the Jurkat T cell model system, expression of a carcinoembryonic Ag-specific CD3ζ CAR (MFEζ) resulted in an increased sensitivity of the transduced Jurkat cell to generate cytokines when stimulated through the endogenous TCR complex. This effect was driven through two key characteristics of the MFEζ CAR: 1) receptor dimerization and 2) the interaction of the CAR with the endogenous TCR complex. Mutations of the CAR transmembrane domain that abrogated these interactions resulted in a reduced functional capacity of the MFEζ CAR to respond to carcinoembryonic Ag protein Ag. Taken together, these results indicate that CARs containing the CD3ζ transmembrane domain can form a complex with the endogenous TCR that may be beneficial for optimal T cell activation. This observation has potential implications for the future design of CARs for cancer therapy. ***The Journal of Immunology*****, 2010, 184: 6938–6949.**

Redirecting T cell specificity through the expression of artificial Ag receptors is currently the source of widespread research and testing in a number of early phase clinical trials worldwide (1, 2). Two basic approaches have been explored to date: first, the expression of α and β TCR chains in the T cell, thereby driving the formation of new TCR complexes with the desired Ag specificity in the gene-modified T cell (3, 4); and second, the expression of receptors bearing T cell signaling receptors fused to extracellular domains that bind to defined target Ags (5). The most commonly explored route for this second group of receptors (chimeric Ag receptors [CARs]) involves the fusion of a single-chain Ab fragment (scFv) to the signaling domain(s). This approach is attractive because the use of scFv to direct the functional response of the T cell against intact cell surface targets means that the CAR$^+$ T cell avoids the requirement of the target cell to process and present peptide Ag—a process frequently dysfunctional in tumor cells and thought to aid the tumors' avoidance of immune surveillance (6–8).

The list of target Ags that have been shown to be suitable for CARs is steadily expanding, indicating the flexible nature of this approach (5). In terms of the signaling domain, there has also been a gradual development of receptor technology moving from "first"-generation receptors, which use a single signaling domain to drive the functional activity of the T cell, through "second"- and "third"-generation receptors, which incorporate additional costimulatory signaling domains that have been shown to result in more potent signaling by the CAR (9, 10). Although the basic elements of the CAR are becoming more clearly understood and engineered for optimal function, however, the structural implications of CAR expression upon the gene-modified T cell remain unknown.

At an early stage, comparisons of first-generation CARs suggested that the CD3ζ-chain was more effective in the CAR format than other signaling domains (11), and this work has largely driven the fact that the CD3ζ-chain is routinely used in the majority of recent CAR designs and is being used in phase I clinical trials of T cells targeting carcinoembryonic Ag (CEA) in colorectal cancer and CD19 in B cell lymphoma. In addition, given the depth of knowledge now available concerning the basic biology of the CD3ζ-chain and its biochemical and molecular interactions with the TCR/CD3 complex, it appeared wise to revisit issues regarding the observed efficiency of the CD3ζ CAR to explore whether lessons from this first-generation receptor may be applicable to the future optimization of CAR design.

Materials and Methods

Abs and cell lines

PE-conjugated anti-human CD3ε (UCHT1), CD28 (CD28.2), CD45RA (HI100), CD69 (FN50), CD95 (DX2), CD107a (H4A3), TCRVβ8 (JR2), anti-mouse CD3ε (145-2C11), PE mouse IgG1, IgG2b, PE hamster IgG1, PE-Cy5 conjugated anti-human CD8 (HIT8A), and anti-human CD3ζ were all purchased from BD Biosciences (Oxford, U.K.). HRP-sheep anti-mouse IgG, FITC- and PE-conjugated goat anti-human IgG, and biotinylated anti-FLAG M2 Abs were purchased from Sigma-Aldrich (Gillingham, Dorset, U.K.). Anti-human IFN-γ (25718.111) and biotinylated anti-human IFN-γ (25723.11) were from R&D Systems (Abingdon, U.K.). The Jurkat cell

*Cell Therapy Group, Cancer Research UK Department of Medical Oncology and §Children's Cancer Group, School of Cancer and Enabling Sciences; and †Advanced Imaging Group and ‡Flow Cytometry Group, Paterson Institute for Cancer Research, University of Manchester, Manchester, United Kingdom

Received for publication June 3, 2009. Accepted for publication April 7, 2010.

This work was supported by the Biotechnology and Biological Sciences Research Council (to J.S.B.); Cancer Research UK (to R.E.H., D.E.G., S.B., M.H., and M.B.); and the European Union Framework Programme 6 Adoptive Engineered T Cell Targeting to Activate Cancer Killing.

Address correspondence and reprint requests to Dr. David E. Gilham, Cell Therapy Group, Cancer Research UK Department of Medical Oncology, Paterson Institute for Cancer Research, Wilmslow Road, Withington, Manchester M20 4BX, U.K. E-mail address: dgilham@picr.man.ac.uk

The online version of this article contains supplemental material.

Abbreviations used in this paper: CAR, chimeric Ag receptor; CEA, carcinoembryonic Ag; FCIP, flow cytometric immunoprecipitation; FRET, Förster resonance energy transfer; MFI, mean fluorescence intensity; NT, nontagged.

line E6-1 was obtained from the European Cell Culture Collection (Porton Down, U.K.). 293T cells were obtained from the American Type Culture Collection. The CEA$^+$ human gastric carcinoma cell line MKN45k has been previously described (12). The mouse MA5.8 cell line was a kind gift from Dr. David L. Wiest (Fox Chase Cancer Center, Philadelphia, PA). Jurkat and MA5.8 cell lines were maintained in T cell media (RPMI 1640 + 10% heat-inactivated FCS, 1% 1M HEPES, 1% L-glutamine and 0.1% 2-ME). MKN45k and 293T cells were maintained in DMEM + 10% FCS.

Generation of CAR constructs

All CAR constructs contain the MFE23 anti-CEA single-chain Ab that has been previously described (12). The MFE.hFc.mtm CAR consists of the murine MHC class I transmembrane domain (aa 210–249) fused to an extracellular human IgG Fc spacer region that has been previously described (13). MFE.hFc.htmζ consists of the same human IgG spacer fused to the human MHC class I truncated extracellular and transmembrane domains (aa 274–313) and human CD3ζ cytoplasmic domain (aa 32–142). MFE.htmζ is identical to MFE.hFc.htmζ but lacks the spacer region. MFE.CD28ζ consists of the entire CD28 molecule (aa 3–202) fused to the CD3ζ cytoplasmic domain (aa 31–142). The CD28 extracellular domain is linked to MFE23 via a pair of GSG flexible linker motifs. All other CARs are based on the MFEζ construct previously described (12) and mutated accordingly (see below).

Mutagenesis of the CAR constructs was carried out using a Site-Directed Mutagenesis kit (Invitrogen, Paisley, U.K.) according to the manufacturer's instructions, using the following primer pairs:

C2G G-10C
For-5′-gccgctacagactgcgcgagctttggcctgctggatcc-3′
Rev-5′-ggatccagcaggccaaagctcgcgcagtctgtagcggc-3′
L9C
For-5′-cccaaactcggctacctgctggatggaatctgcttcatctatggtg-3′
Rev-5′-caccatagatgaagcagattccatccagcaggtagccgagtttggg-3′
C2G G7C
For-5′-gctggatcccaaactcggctacctgctggattgcatcctcttcat-3′
Rev-5′-atgaagaggatgcaatccagcaggtagccgagtttgggatccagc-3′
C2G G13C
For-5′-cggctacctgctggatggaatcctcttcatctattgtgtcattctcactgc-3′
Rev-5′-gcagtgagaatgacacaatagatgaagaggattccatccagcaggtagccg-3′
D6K
For-5′-ggatcccaaactctgctacctgctgaagggaatcctcttcatctatggtgtc-3′
Rev-5′-gacaccatagatgaagaggattcccttcagcaggtagcagagtttgggatcc-3′
F10A
For-5′-atggaatcctcgccatctatggtgtcattctcactgccttgttcc-3′
Rev-5′-ggaacaaggcagtgagaatgacaccatagatggcgaggattccat-3′.

Alternatively, for the D6N, D6E, and D6Q amino acid substitutions, mutations were introduced using PCR to take advantage of a BamHI site 5′ to the D6 codon. To this end, forward primers were generated containing the relevant mutation plus a BamHI site, which was used along with a CD3 reverse primer. Following amplification, the mutant sequence was ligated into rKat.om1.MFE23.CD3ζ via a BamHI/blunt ligation. MFE.C2Gζ was amplified using a forward primer containing the relevant mutation at the 3′ end and a 5′ NotI site, which was used alongside the CD3 reverse primer. Following amplification, the product was inserted into rKat.om1.MFE23.CD3ζ via a NotI/blunt ligation.

CD3: Rev-5′-tctagattattagcgaggggcagggcctgcatgt-3′
NotI C2G: For-5′-gcggccgctacagacggagcgagctttggcctgctggatcccaaactcggctacc-3′
BamHI D6E: For-5′-ggatcccaaactctgctacctgctggagggaatcctcttcatct-3′
BamHI D6N: For-5′-ggatcccaaactctgctacctgctgaatggaatcctcttcatc-3′
BamHI D6Q: For-5′-ggatcccaaactctgctacctgctgcagggaatcctcttc-3′

For generation of FLAG-tagged receptors, MFEζ was PCR amplified to remove the 3′ stop codons and a SalI site was introduced directly after the CD3ζ sequence, using the CD3 SalI Rev primer. This product was first subcloned into the multiple cloning site of pFLAG-CMV-5a vector (Sigma-Aldrich) via a NotI/SalI ligation and then used as a template for a subsequent PCR, using the FLAG XhoI Rev primer, which introduced a 3′ XhoI site. This product was then cloned into the rKat vector via a NotI/XhoI–SalI ligation, which removed the original SalI site, thus permitting additional CAR sequences to be introduced into the expression cassette downstream of the FLAG sequence via NotI/SalI ligations.

CD3 SalI: Rev-5′-gtcgacgcgaggggcagggcctgcat-3′
FLAG XhoI: Rev-5′-ctcgagttattacttgtcatcgtcgtccttg-3′

Retrovirus generation and lymphocyte transduction

The rKat retroviral vector system was used as previously described (14). Retroviral supernatant was produced from transiently transfected 293T cells, using a modified calcium chloride transfection protocol, which has been previously described (12). Media from 293T cells were filtered through a 0.45 μM filter and used to directly infect Jurkat T cells. Briefly, 5×10^5 Jurkat T cells were mixed with retroviral supernatant plus 6 μg/ml polybrene and centrifuged for 3 h at $1200 \times g$. Transductions were repeated on 2 consecutive days. For primary human T cell analysis, buffy coats were activated for 24 h with 30 ng/ml OKT3 and anti-CD28 plus 100 IU/ml IL-2. Following activation, cells were transduced directly in a coculture with transfected 293T cells or spinfected as for Jurkat T cells. Cells were expanded for 2 wk. CAR-expressing T cells were isolated using CEAhFc/anti-hIgG PE plus anti-PE microbeads (Miltenyi Biotec, Surrey, U.K.). Enriched cells were mixed with 2×10^7 4 Gy irradiated allo buffy coat feeders plus anti-CD3/CD28 + Il-2 and expanded for an additional 2 wk prior to functional assays.

Flow cytometric analysis and FACs sorting

Transduction levels of all cells were assessed using CEAhFc protein generated from transiently transfected 293T cells, as previously described (13). Cells were incubated with CEAhFc for 30 min on ice, followed by incubation with anti-human IgG-PE Abs. FACS analysis was conducted using either a FACScan or a FACSCalibur flow cytometer (BD Biosciences) and WinMDI 2.8 software. FACS sorting was performed using a FACSVantage or FACSAria cytometer. Populations were sorted to obtain cells with equivalent CAR surface expression (generally the top 5% of expressers).

Flow cytometric immunoprecipitation

Streptavidin-coated polystyrene beads of 6.0–8.0 μm (Spherotech, Lake Forest, IL) were coupled to biotinylated anti-FLAG M2 Abs (Sigma-Aldrich) according to the manufacturer's instructions. Next, 100 μl beads was incubated with 500 μg cell lysate from Jurkat T cells treated with 0.5% Brij lysis buffer (0.5% Brij-98 [Sigma-Aldrich]; 20 mM TrisHCl, pH 8; 137 mM NaCl; 2 mM EDTA; 10% glycerol; 500 μM sodium orthovanadate; 1 mM sodium fluoride; and protease inhibitor tablets according to the manufacturer's instructions [Roche, Burgess Hill, West Sussex, U.K.]). Following 30 min incubation at 4°C, the beads were washed twice with 1% BSA/PBS and incubated for 30 min with CEAhFc or anti-TCRVβ8-PE Abs, or an appropriate isotype control. Samples incubated with CEAhFc were washed as previously and incubated with anti-human IgG-PE secondary Abs for an additional 30 min. Following staining, the beads were washed twice as previously and finally resuspended in 200 μl 1% paraformaldehyde/PBS. Beads were analyzed using an LSRII flow cytometer (BD Biociences) and FACSDiva software. Data were analyzed using FlowJo software (Tree Star, Ashland, OR), and geometric mean values were obtained for each sample and compared against equivalent isotype-matched control samples.

Förster resonance energy transfer

Forward (5′-gaattcaccatggagtctccctcggcccctccccacagatggtgc-3′) and reverse primers (5′-gtcgacgcaatagaggacattcaggatgactgaatcactgcgcctggcactc-3′) were designed to amplify the CEA sequence from the N terminus, without the leader sequence, to the C terminus of the first loop containing the epitope for the MFE23 ScFv (designated tCEA). The amplified product terminated at the codon for W235. The primer was designed to clone a 3′ cysteine that was hypothesized to increase fluorochrome conjugation. The forward primer contained an NheI site, and the reverse primer contained an XbaI site, which allowed cloning of the product into the pFLAG-CMV-5a plasmid (Sigma-Aldrich). The product was first subcloned into the TOPO vector for sequence confirmation before subsequent cloning into pFLAG-CMV-5a. 293T cells were transiently transfected with the plasmid, and the media were pooled and filtered through 0.2-μm filters 48 and 72 h later. Column chromatography was carried out using the Mammalian Carboxy-Terminal FLAG Transient Expression kit (Sigma-Aldrich) according to the manufacturer's instructions. The tCEA proteins were eluted under acidic conditions, using 0.1 M glycine, pH 3.5. Fractions were collected and analyzed using a NanoDrop (Wilmington, DE) spectrophotometer at A280. Fractions containing protein were pooled and dialyzed overnight against PBS. Successful protein purification was assessed by staining of CAR-expressing Jurkat T cells with purified protein.

Dialyzed tCEA protein was filter sterilized and then concentrated using a Centricon Centrifugal Filter Unit with an Ultracel YM-10 membrane (Millipore, Billerica, MA) according to the manufacturer's instructions. Fluorochrome conjugation of tCEA+C and anti-TCRVβ8 Abs using Alexa Fluor

555 and Alexa Fluor 647 Microscale Protein Labeling kit (Molecular Probes/Invitrogen, Eugene, OR) were carried out according to the manufacturer's instructions. Conjugation of mouse anti-human TCRVβ8 mAb was performed using Alexa Fluor 555 and Alexa Fluor 647 mAb Labeling kits (Molecular Probes/Invitrogen) according to the manufacturer's instructions.

A total of 1×10^5 transduced Jurkat T cells were stained with Alexa Fluor conjugated tCEA and anti-human TCRVβ8 Abs on ice and adhered to slides coated with polylysine (Sigma-Aldrich). Cells were fixed and coverslipped using ProLong Gold anti-fade reagent (Molecular Probes/Invitrogen) and visualized using an Axiovert 200M microscope (Carl Zeiss, Welwyn Garden City, Hertfordshire, U.K.). FRET was analyzed with Metamorph software (Molecular Devices, Sunnyvale, CA) and images merged using Photoshop software. Cells were considered FRET positive when clearly identifiable regions of the processed images constituted the required blue/white shade associated with FRET signals.

PAGE and Western blotting

A total of 1×10^7 cells were lysed in 300 μl 1% CHAPS buffer (PBS, 1% CHAPS, 0.5% sodium deoxycholate, 2% $NaDodSO_4$, plus protease inhibitor tablet [Roche]) for 30 min and then centrifuged through polymer wool to clear the supernatant. Samples containing equal numbers of cells were mixed 1:1 with reducing or nonreducing loading buffer and boiled for 5 min or left untreated, respectively. All lysates were separated on 10% SDS-PAGE gels, transferred to Hybond nitrocellulose membrane (Amersham Biosciences, Little Chalfont, Buckinghamshire, U.K.), and probed with 1:1000 dilution of mouse anti-human CD3ζ mAb and 1:1000 dilution of sheep anti-mouse HRP-conjugated IgG diluted in PBS-Tween/5% skimmed milk powder. Bands were resolved using the ECL Western Blotting Detection kit (Amersham Biosciences) according to the manufacturer's instructions, and the membranes were analyzed by exposure to X-ray film (Kodak, Rochester, NY).

For native gel analysis, Jurkat T cells were lysed in 1% digitonin buffer (1.0% digitonin [Sigma-Aldrich]; 20 mM TrisHCl, pH 8; 137 mM NaCl; 2 mM EDTA; 10% glycerol; 500 μM sodium orthovanadate; 1 mM sodium fluoride; and protease inhibitor tablets according to the manufacturer's instructions [Roche]). Then 60 μg total protein was separated on 4–15% Tris-Glycine gels (Bio-Rad, Hercules, CA). Protein was transferred to membranes and probed with Abs, as indicated.

ELISA

Matched-pair anti-human IFN-γ mAbs were used according to the manufacturer's instructions (R&D Systems). Standards were obtained from R&D Systems and were added in triplicate at doubling dilutions to produce a standard curve (2000 pg/ml–15.6 pg/ml). Control samples were added in triplicate.

CD107a cytotoxicity assay

MKN45k cells were mixed at an effector/target ratio of 1:1 in the presence of GolgiStop (BD Biosciences) for 4 h. Following coculture, cells were stained with PE anti-CD107a, PE-Cy5 anti-CD8, and CEAhFc/anti-hIgG-FITC Abs and were analyzed using a FACSCalibur cytometer.

CD69 expression assay

Ninety-six-well flat-bottom non–tissue-culture-treated plates were coated overnight with doubling dilutions (1.0 μg/ml–0.004 μg/ml) of CEA protein diluted in borate buffer. Next day, the plates were blocked for 1–2 h at 37°C with 2% BSA/PBS before the addition of 1×10^5 Jurkat T cells in a total volume of 100 μl T cell media per well. Plates were incubated for 24 h at 37°C before cells were collected, stained with anti-CD69 Abs, and analyzed using a FACScan or FACSCalibur cytometer.

Statistical analysis

Upregulation of CD3ε in Jurkat T cells was analyzed using a nonparametric Kruskal–Wallis test with significance indicated to either $*p < 0.05$ or $**p < 0.01$. For analysis of differences in EC_{50} values, two-way ANOVA was applied with a post hoc Dunnet test compared against the indicated control with the same significance levels as indicated above.

Results

CARs containing the CD3ζ transmembrane domain induce upregulated expression of CD3ε in Jurkat T cells

Given the recent developments of CAR technology, a series of CEA-specific receptors [using the MFE23 scFv (12, 13)] were generated that bore differing transmembrane and signaling domains to explore the differences in activity between these receptor formats (Fig. 1*A*). To facilitate the rapid testing of these constructs, Jurkat E6-1 T cells were transduced and cell sorted to achieve cell populations with approximately equivalent levels of CEA binding potential (Fig. 1*A*) As expected, only the Jurkat T cells harboring an anti-CEA CAR responded to CEA protein Ag (Fig. 1*B*). Although MFE.hFc.htmζ did not demonstrate detectable levels of CEA-specific IFN-γ release, this particular receptor could drive low levels of CD69 upregulation (Supplemental Fig. 1*A*) following Ag challenge, suggesting that the hFc spacer may be reducing the overall capacity for the receptor to function; indeed, this reflects previous observations suggesting that extracellular spacer regions adversely impact upon the function of the MFE23 scFv in a chimeric receptor format (13). Somewhat surprisingly, the Jurkat T cell populations engrafted with the CD3ζ chimeric receptor (hereafter termed MFEζ) produced significantly greater quantities of IFN-γ upon polyclonal stimulation with mitogenic Abs specific for CD3ε (either alone or in combination with anti-CD28) than all of the other cell populations (Fig. 1*B*). This effect was consistent across a number of independent transduction and sorting experiments, indicating that the effect was not likely to be due to an effect of retroviral transduction or cell sorting. A potential reason for this effect was an apparent increase in the level of CD3ε expression on the surface of the MFEζ CAR cells (Fig. 1*C*). However, CD28 expression in the various cell populations was equivalent, suggesting that the MFEζ CAR was not driving a global increase in cell surface protein expression (Fig. 1*C*).

Dimerization of the MFEζ CAR is important for sensitivity to CEA protein Ag

This observation suggests that the CAR may be interacting with elements of the TCR/CD3 complex. Previous work using CD3ζ CARs demonstrated that the receptor could form heterodimers with endogenous CD3ζ by immunoblotting (12, 15, 16). Dimerization of CD3ζ is thought to be predominantly driven by disulfide bonding through a single cysteine residue (Cys) on the external edge of the CD3ζ transmembrane domain (17). Consequently, a MFEζ receptor was generated whereby this cysteine was mutated to glycine to generate the MFE.C2Gζ receptor. As a nondimerizing receptor control, a CAR receptor containing the human HLA-A2 transmembrane domain (MFE.htmζ) was generated, and Jurkat cells were transduced and sorted to generate cell populations with similar CEA binding ability (Fig. 2*A*) and similar levels of chimeric receptor protein expressed (Fig. 2*B*). Nonreduced immunoblots of the sorted Jurkat T cells confirmed that the MFEζ receptor existed as heterodimers with endogenous CD3ζ and homodimers with the MFEζ CAR, whereas the MFE.C2Gζ and MFE.htmζ were both unable to dimerize as expected (Fig. 2*C*). Furthermore, neither of the nondimerizing receptors could upregulate expression of CD3ε, compared with the MFEζ receptor (Fig. 2*D*). To test the functional response of the cell lines, the T cells were tested for the ability to upregulate CD69 in response to Ag stimulus provided in the form of various concentrations of plate-bound CEA protein. The MFEζ receptor proved to be the most efficient receptor of the three tested in that it required the lowest coating concentration of CEA to achieve 50% maximal CD69 expression (0.03 ± 0.01 μg/ml, Fig. 2*E*). The MFE23.htmζ receptor required a 10× higher coating concentration of CEA to achieve this level of CD69 expression, whereas the MFE.C2Gζ appeared intermediate to both (Fig. 2*E*).

To further explore the role of dimerization in optimal CAR function, mutations were introduced into the MFE.C2Gζ receptor to introduce cysteine residues at sites within the transmembrane

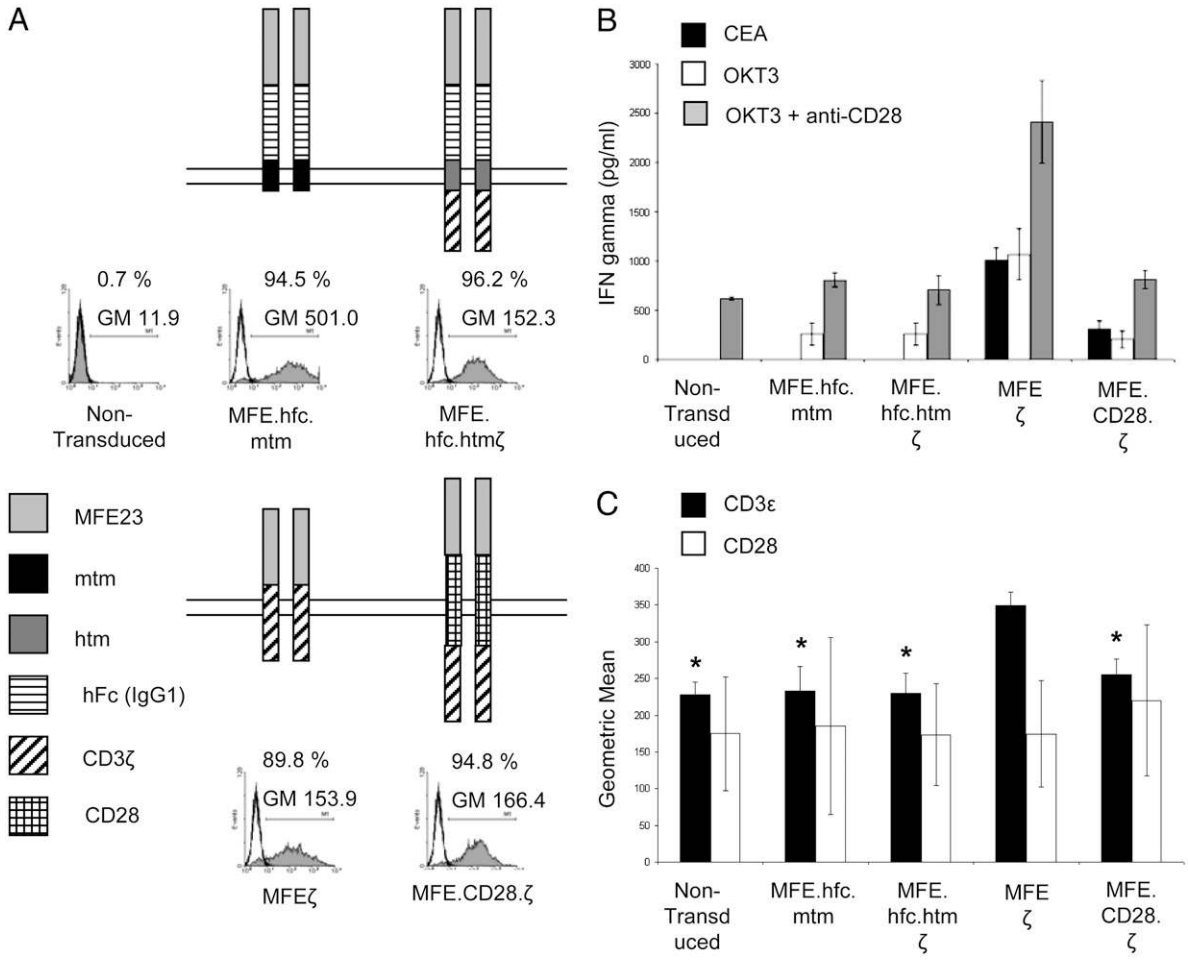

FIGURE 1. CD3ζ transmembrane domain-containing CARs induce a functional upregulation of CD3ε in Jurkat T cells. Jurkat T cells were transduced with retroviruses encoding CAR constructs with varying modular structures and were FACS sorted to obtain populations with relatively equal surface expression (*A*). Transduced Jurkat T cells were stimulated with 1.0 μg/ml immobilized CEA, 1.0 μg/ml immobilized OKT3, or 1.0 μg/ml immobilized OKT3 + 1.0 μg/ml immobilized anti-CD28 Abs for 24 h. Media from incubations were analyzed for IFN-γ secretion by ELISA (*B*). CD3ε and CD28 were analyzed by flow cytometry and geometric mean values compared (*C*). $*p < 0.05$ by Kruskal–Wallis test. Data represent mean ± SD of triplicates in an experiment representative of three independent experiments (*B*) or mean ± SD from three independent analyses (*C*).

region thought to potentially be suitable for receptor dimerization (refer to Fig. 3*A*). Of the receptors produced, those with the cysteine introduced within the CD3ζ transmembrane domain (G13C, L9C, and G7C) failed to generate dimers at all (Fig. 3*B*). Only when the cysteine was located on the extracellular aspect of the receptor (G-10C) was receptor dimerization observed (Fig. 3*B*). In the CD69 upregulation assay, the monomeric receptors displayed Ag responsiveness that was similar to that of the MFE.C2Gζ receptor, except for the L9C receptor, which responded extremely poorly to Ag (Fig. 3*C* and Supplemental Fig. 1*B*). However, the G-10C receptor showed an enhanced sensitivity to Ag when compared with the MFE.C2Gζ receptor, although this level of sensitivity was still significantly less efficient than the parental wild-type MFEζ (Fig. 3*C*, 3*D*). These observations were confirmed by IFN-γ secretion in primary human T cells (Supplemental Fig. 3*A*). IFN-γ secretion by the monomeric receptors (MFE.C2Gζ and MFE.htmζ) was severely abrogated in response to CEA compared with MFEζ. Furthermore, redimerization did not recapitulate optimal activity.

These results demonstrated that dimerization of the MFEζ CAR is an important determinant for optimal Ag sensitivity. However, the loss of the disulfide bridge alone in the MFE.C2Gζ failed to reduce the responsiveness of this receptor to the level of the receptor lacking a CD3ζ transmembrane domain, suggesting that other factors that influence the Ag sensitivity of the CD3ζ CAR may be at play.

Mutations to the CD3ζ transmembrane D6 residue severely impact on CAR function

Aside from the dimerizing disulfide bridge motif, molecular analysis of the CD3ζ-chain has indicated that charged residues within the transmembrane domain mediate ionic interactions with other members of the TCR/CD3 complex (18, 19). In particular, an aspartic acid residue (D6; refer to Fig. 3*A*) is thought to play an important role in CD3ζ dimerization and in stabilizing the TCR/CD3 complex through interaction with basic lysine residues on the TCRα-chain (20, 21). We questioned whether mutating this aspartic acid in the MFEζ CAR in a manner similar to that used in experiments with wild-type CD3ζ-chain (18) impacted upon CAR function. Mutant receptors bearing conservative acidic–acidic mutations (D6E), acidic–neutral mutations (D6N or D6Q), or acidic–basic mutations (D6K) were generated, and Jurkat T cell populations were generated for functional analysis.

Under reducing immunoblot conditions, all receptors appeared as single immune reactive bands of similar m.w. (Fig. 4*A*). Under nonreducing conditions, CARs carrying the D6E or D6N mutations exhibited comparable levels of hetero- and homodimerization, as seen in the MFEζ receptor (Fig. 4*B*). However, the D6Q mutation partially inhibited dimer formation, whereas the D6K mutation abrogated dimer formation to a much greater level (Fig. 4*B*). Each

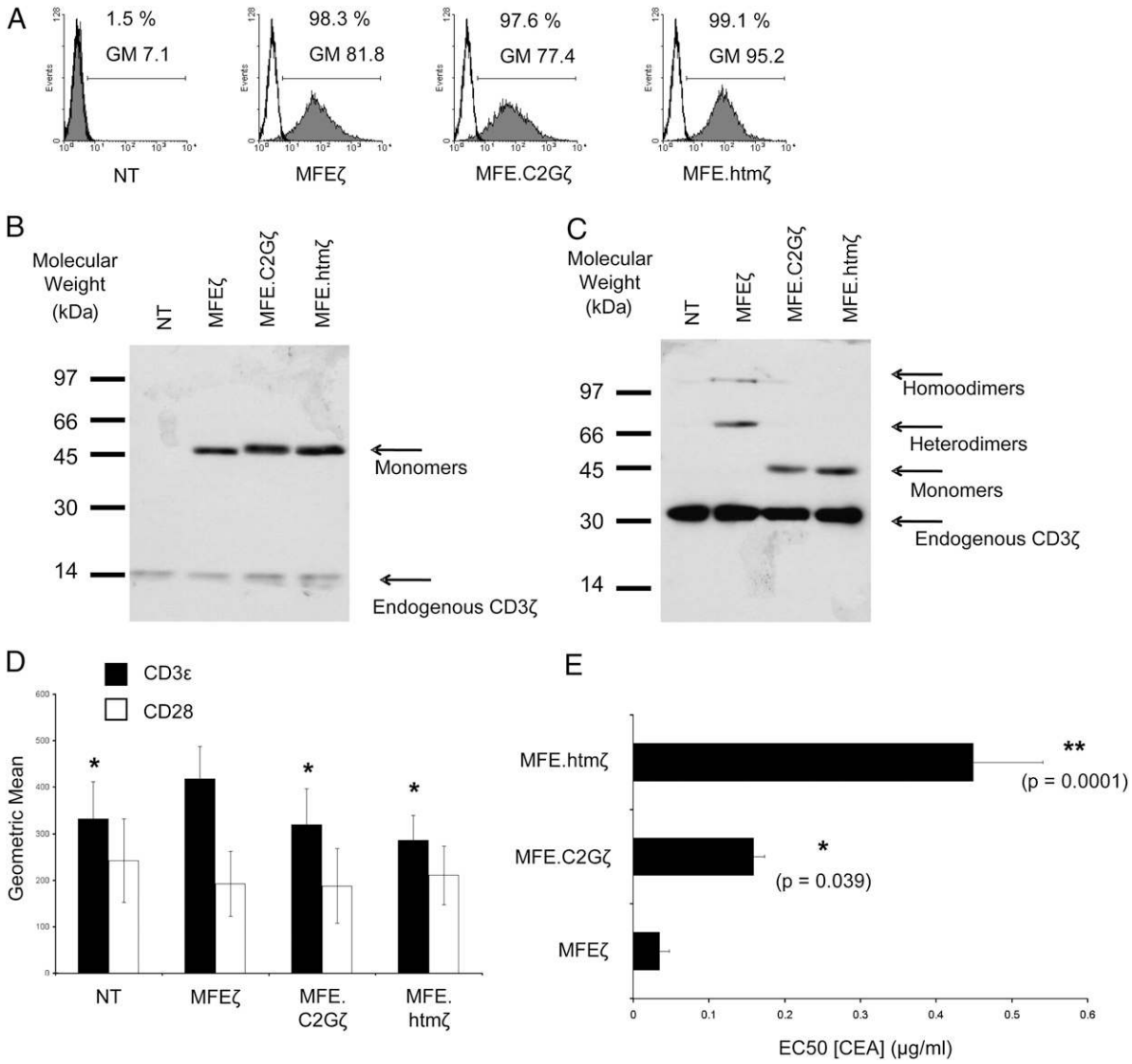

FIGURE 2. Inhibition of CAR dimerization abrogates upregulation of surface CD3ε and has a negative impact on CAR Ag sensitivity. Jurkat T cells were retrovirally transduced with vectors encoding the wild-type MFEζ CAR or mutant receptors containing either a C2G mutation in the transmembrane domain (MFE.C2Gζ) or a heterologous nondimerizing transmembrane domain MFE.htmζ and were sorted to obtain populations with relatively equal surface expression (*A*). Reducing (*B*) and nonreducing (*C*) immunoblot analysis of CAR-engrafted Jurkat T cell lysates. CD3ε and CD28 expression was analyzed by FACS (*D*). Transduced cells were incubated on immobilized CEA for 24 h before staining with CD69 Abs and analysis by flow cytometry. The concentration of CEA required to achieve 50% maximal CD69 expression in OKT3-activated Jurkat T cells was calculated (*E*). $*p < 0.05$; $**p < 0.01$ compared with MFEζ by Kruskal–Wallis test (*D*) or Student *t* test (*E*). Data represent mean ± SD from three (*E*) or six (*D*) independent analyses.

of the mutants showed an abrogated CD69 response to immobilized CEA protein when compared with MFEζ, although differences existed depending on the mutation present, with the rank order of potency being D6N > D6E = D6Q > D6K (Fig. 4*C* and Supplemental Fig. 1*C*). The results from Jurkat T cells were confirmed in primary human T cells. We found that the MFEζ$^+$ cells exhibited a higher CD3ε mean fluorescence intensity (MFI) than did the untransduced population (Supplemental Fig. 3*D*). In comparison, cells expressing any other receptor did not show an increased tendency to upregulate CD3ε in the CAR$^+$ population. Indeed, cells expressing the D6Q variant demonstrated a marked downregulation in CD3ε (MFI: 12.4 compared with 78.2 in the MFEζ CAR$^+$ population). IFN-γ secretion in response to immobilized CEA was also analyzed with a D6N mutation abrogating IFN-γ secretion in response to CEA compared with MFEζ. As observed in Jurkat T cells, D6E and D6Q mutations induced a more severe effect on activity than did the D6N mutation (Supplemental Fig. 3*B*). Cytotoxic cell function, as measured by CD107a upregulation (increase in MFI values) in response to CEA-expressing tumor cells, demonstrated a similar pattern: Mutations to the D6 residue impacted on MFEζ in the relative order D6N > D6E > D6Q > D6K, with mutations affecting the dimerization status also abrogating degranulation (Supplemental Fig. 3*C*).

These data suggest that the D6 residue is important for optimal CD3ζ CAR function and further suggest that the overall charge of this residue is important. To confirm that any mutation to the transmembrane domain did not abrogate MFEζ function, a receptor bearing a F10A mutation that was predicted to have no effect upon function was generated and shown to form stable hetero- and homodimers like MFEζ (Supplemental Fig. 2*A*) and to have no effect on CAR activity (Supplemental Fig. 2*B*).

The combination of C2G and D6K mutations dramatically reduces the Ag sensitivity of the MFEζ CAR

Given the observations that two individual amino acid changes alone had a detrimental effect upon the MFEζ CAR, we questioned

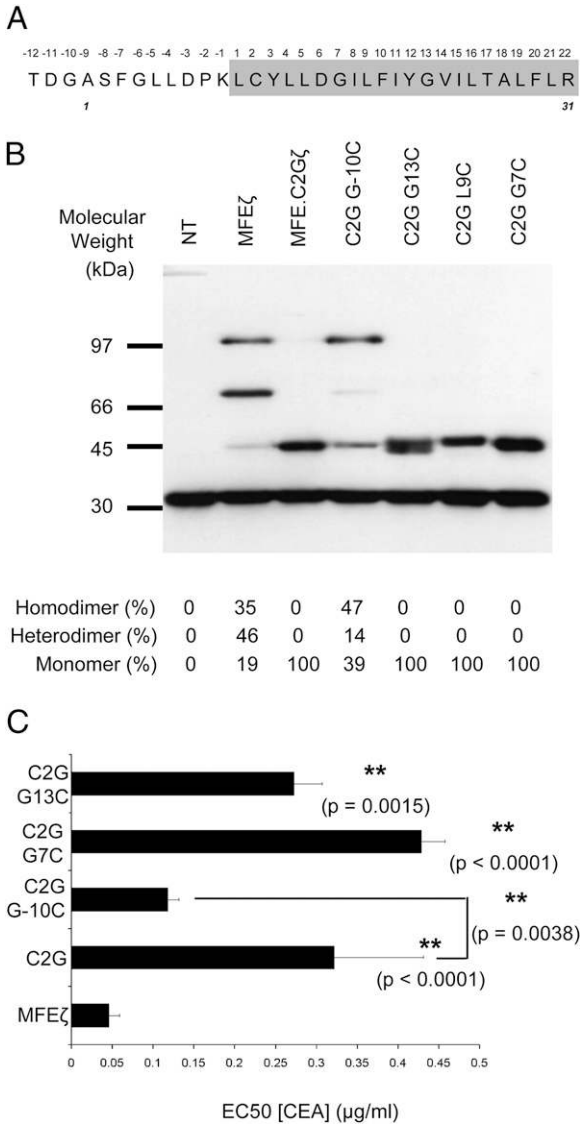

FIGURE 3. Redimerization of the MFE.C2Gζ CAR partially restores optimal Ag sensitivity. Cysteine residues were introduced into novel positions in the transmembrane (position 7, 9, or 13) or extracellular domains (position −10 relative to transmembrane domain) of MFE.C2Gζ, to attempt redimerization. The amino acid sequence of human CD3ζ used in MFEζ is shown with the transmembrane domain highlighted (*A*). Numbers above refer to the amino acids relative to the transmembrane domain and are those used in this paper. Numbers below refer to the amino acid sequence relative to full-length human CD3ζ. *B*, Nonreducing immunoblot analysis of Jurkat T cell lysates. Ag sensitivity of CARs was assessed by incubating transduced cells on immobilized CEA for 24 h before staining with anti-CD69 Abs and analysis by flow cytometry (*C*). CEA EC_{50} values were calculated for each CAR (*D*). $*p < 0.05$; $**p < 0.01$ by two-way ANOVA with a post hoc Dunnet test compared with MFEζ unless shown. Ag sensitivity assays show mean ± SD from three independent experiments.

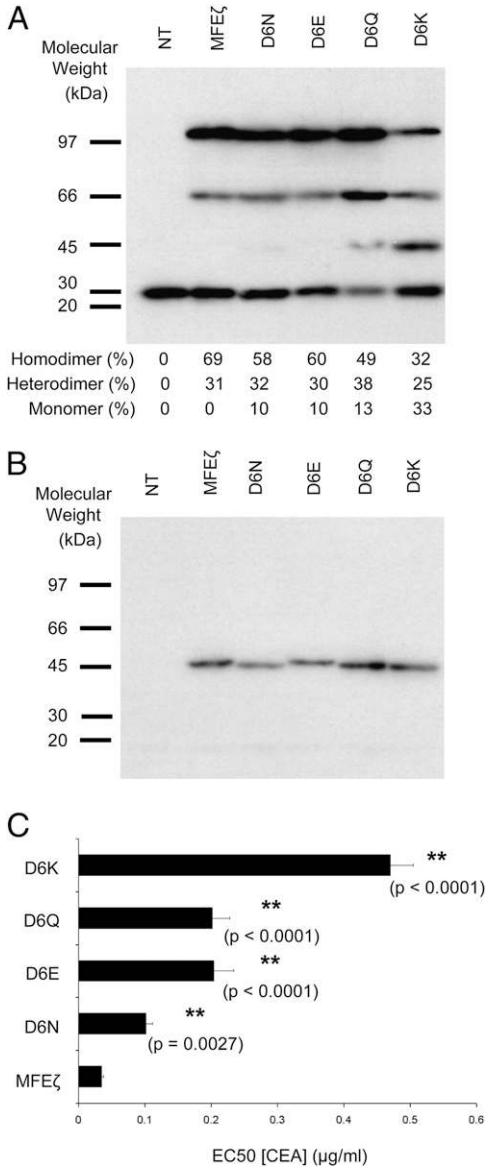

FIGURE 4. Mutations to the charged transmembrane aspartic acid residue affect CAR dimerization and Ag sensitivity. Mutations were introduced at the transmembrane D6 residue (D6N, D6E, D6Q, D6K), and Jurkat T cells were retrovirally transduced with vectors encoding these mutant receptors. Nonreducing (*A*) and reducing (*B*) immunoblot analysis of D6 mutant CAR-engrafted Jurkat T cell lysates. CAR-engrafted Jurkat T cells were incubated on immobilized CEA for 24 h before staining with anti-CD69 Abs and analysis by flow cytometry (*C*). EC_{50} values were calculated for each CAR (*D*). $**p < 0.01$ compared with MFEζ by two-way ANOVA with a post hoc Dunnet test. Ag sensitivity assays show mean ± SD from four independent experiments.

whether the combination of both mutations was sufficient to reduce the Ag sensitivity of this CAR to that of the MFE.htmζ receptor (Fig. 2*E*). The C2G.D6K receptor failed to form dimers as predicted (Fig. 5*A*, 5*B*), and the upregulation of CD69 in response to CEA protein was severely reduced over and above that seen for either mutant receptor alone (Fig. 5*C* and Supplemental Fig. 1*D*). Taken together, this mutational analysis strongly indicates that two amino acid residues thought to be important for the biological function of wild-type CD3ζ are also critical determinants for the optimal function of a CD3ζ-containing CAR.

The MFEζ CAR can rescue the cell surface expression of TCR/CD3 complexes in CD3ζ-deficient MA5.8 cells

Initial experiments demonstrated that the expression of the MFEζ CAR in Jurkat T cells resulted in increased cell surface expression of CD3ε (Fig. 1*C*). It is known that CD3ζ is a key limiting factor that controls the progression of intact TCR/CD3 complexes to the cell surface (22, 23). Consequently, it is possible that the MFEζ CAR may be providing an additional source of CD3ζ, which in turn permits an increased level of cell surface TCR/CD3 complex. As such, it was important to determine whether the CAR interacts strongly within the TCR/CD3 complex in a manner similar to that

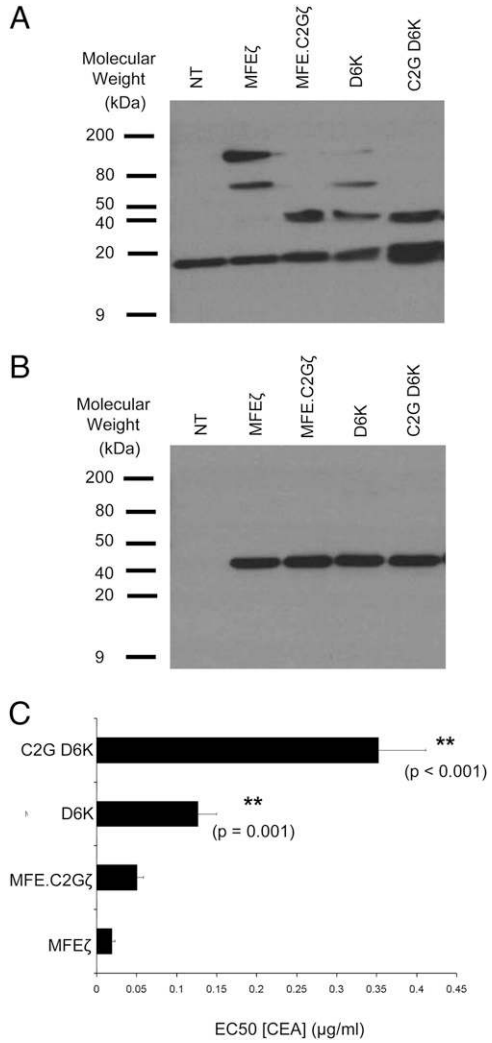

FIGURE 5. Combined C2 and D6 mutations further abrogate CAR Ag sensitivity. A mutant receptor containing a combination of C2G and D6K transmembrane mutations was cloned. Cells were transduced with this double mutant receptor or previously described wild-type MFEζ, MFE.C2Gζ or D6K CAR. Nonreducing (*A*) and reducing (*B*) Western blot analysis of CAR-engrafted Jurkat T cell lysates. CAR-engrafted Jurkat T cells were incubated on immobilized CEA for 24 h before staining with anti-CD69 Abs and analysis by flow cytometry (*C*). EC_{50} values were calculated for each CAR. $*p < 0.05$; $**p < 0.01$ compared with MFEζ by two-way ANOVA with a post hoc Dunnet test. Ag sensitivity assays show mean ± SD from three independent experiments.

of wild-type CD3ζ. The mouse cell line MA5.8, which lacks endogenous CD3ζ (23), was initially used to test whether the MFEζ CAR could rescue TCR/CD3 expression in this cell line. Indeed, when MA5.8 cells were transduced with the MFEζ receptor, high levels of endogenous TCR/CD3 complex could be detected on the cell surface, strongly suggesting that this CAR could substitute for wild-type CD3ζ in the formation of complete TCR/CD3 complexes (Fig. 6*A*, 6*B*). In approximate agreement with previous biochemical analysis, the MFE.htmζ receptor showed little ability to support the expression of TCR/CD3 complexes in transduced MA5.8 cells. Of the mutated receptors, all showed a reduced ability to restore TCR/CD3 expression in MA5.8 cells, compared with the MFEζ CAR (Fig. 6*A*, 6*B*). Interestingly, the MFE.C2G G-10C receptor with the displaced disulfide bridge, which had demonstrated an enhanced response to Ag, compared with the MFE.C2G.ζ receptor, failed to restore TCR/CD3 expression in this model above that of the C2G.ζ receptor (Fig. 6*A*, 6*B*).

To account for any gross differences in MFI values observed with the different receptors, MFEζ CARs expressing MA5.8 cells were sorted to obtain populations with different surface expression values. The differences in CD3ε MFI were observed despite cell sorting, suggesting that the transmembrane mutations affect surface expression in this cell line. Fig. 6*C* demonstrates that there is a linear correlation between MFEζ expression and TCR reconstitution. Even at low MFI values, MFEζ-mediated TCR reconstitution was significantly higher than that for any of the other mutants tested ($p = 0.0055$ versus MFE C2Gζ and $p < 0.001$ for all others).

Analysis of the F10A mutant, which expressed to the same level as the other receptors tested (Supplemental Fig. 2*C*), indicated that this mutation did not have as significant an abrogation on TCR reconstitution as any of the other mutants receptors tested (Supplemental Fig. 2*D*).

The MFEζ CAR closely interacts with the endogenous TCRβ in Jurkat T cells

The combined cellular-based evidence indicated that the MFEζ was interacting with elements of the TCR/CD3 complex. The various mutations tested suggested that dimerization with endogenous CD3ζ was important; however, the charged amino acid residues within the CD3ζ transmembrane domain also mediate ionic interactions with other components of the TCR/CD3 complex, including the TCRα-chain. To determine whether the MFEζ CAR was also interacting with the TCR, FRET and immunoprecipitation analysis were performed.

Confocal microscopy-based FRET was performed on Jurkat T cell populations expressing either MFEζ or MFE.htmζ, as these receptors appeared to demonstrate the two extremes of CAR–TCR/CD3 interactions (e.g., Fig. 6*B*). FRET was conducted between the CAR and TCRβ-chain. Abs to the TCRβ-chain were chosen, as the βV8 isoform in Jurkat cells has been characterized and TCRα Abs against the TCR C region gave poor signals by flow cytometry. A positive FRET signal between a truncated CEA protein Ag and anti-TCRβ was found in 51% of MFEζ-expressing Jurkat cells, compared with only 14% of MFE.htmζ cells (Fig. 7*A–C*). A positive FRET signal was detected only when the truncated CEA Ag was labeled with Alexa Fluor 647 and the anti-TCR mAb with Alexa Fluor 555. When the Ag/Ab combination was labeled with the reverse fluorophores, no FRET signal was detected in either cell population (Fig. 7*C*). This phenomenon is most likely related to differences in donor/acceptor ratios required for optimal FRET signals in clustered molecules (24). The positive FRET signal strongly suggested that the MFEζ CAR and TCRβ-chain were in close proximity on the surface of transduced Jurkat T cells.

The gold standard biochemical measure of protein–protein interactions is immunoprecipitation. Standard techniques to analyze the CAR–TCR interaction proved unsuccessful, so this led to the development of a novel bead-based flow technique (FCIP) that we have recently reported on (25). A C-terminal FLAG tag was cloned onto the CAR, and Jurkat T cells were transduced and sorted. C-terminal FLAG-tagged receptors responded to CEA in a dose-dependent manner in a highly similar manner to their non–FLAG-tagged counterparts, with similar EC_{50} values observed (Fig. 8*A*).

The FCIP method involved incubating Brij lysates prepared from Jurkat T cells with polystyrene beads coupled to anti-FLAG Abs. These beads were probed with fluorochrome-conjugated Abs to the TCR complex, washed extensively, and then analyzed by flow cytometry (see Fig. 8*B* for example plots for all constructs). To control for CAR binding to the beads, lysate-incubated beads were incubated with CEA protein Ag fused to human IgG_1 Fc (hFc) and a fluorochrome-conjugated anti-hFc mAb.

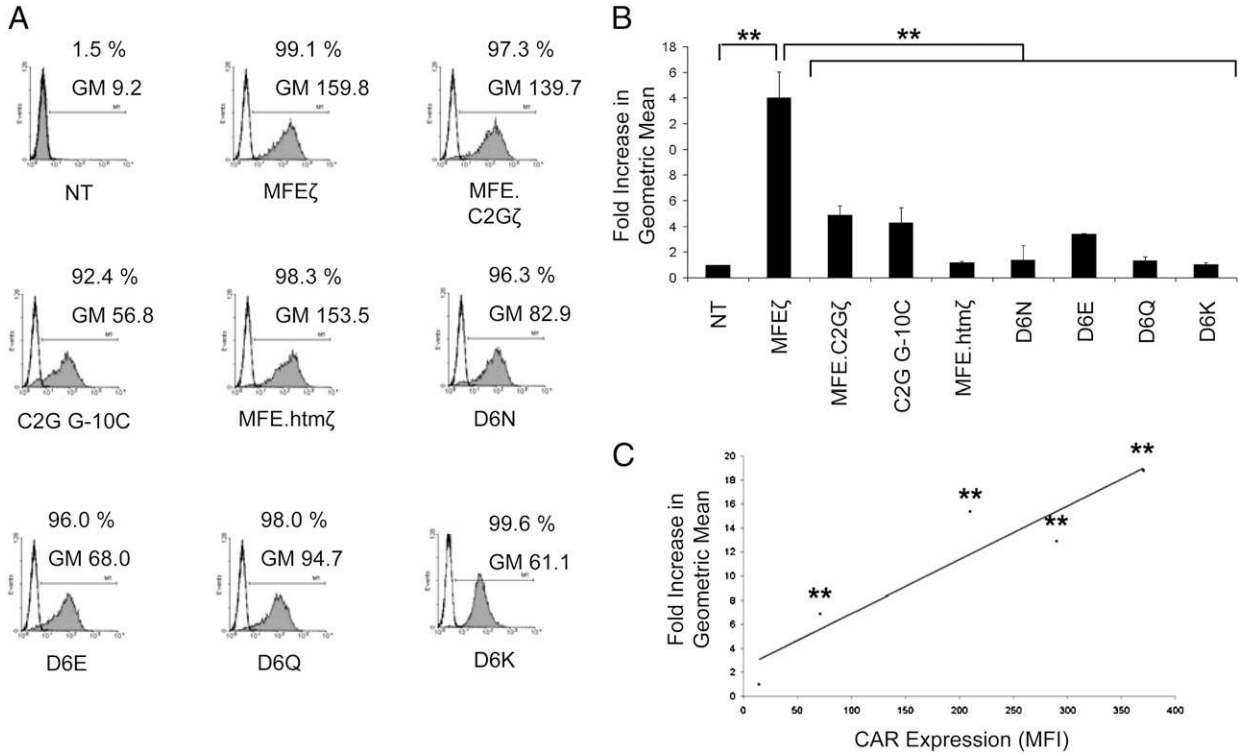

FIGURE 6. MFEζ induces an upregulation of surface TCR complexes in MA5.8 cells. CD3ζ-deficient MA5.8 cells were transduced with a panel of mutant CAR receptors and FACS sorted to obtain populations with relatively equal surface expression (*A*). Transduced MA5.8 cells were stained for surface expression of the TCR component CD3ε and analyzed by flow cytometry. Geometric mean values were compared against nontransduced cells (*B*). MFEζ CAR-expressing cells were sorted to obtain populations with different surface expression values, and TCR reconstitution was assessed (*C*). $*p < 0.05$; $**p < 0.01$ by two-way ANOVA with a post hoc Dunnet test. Data represent mean ± SD from three independent experiments.

When tested using lysates from MFEζ Jurkat T cells, a clear signal for TCR binding was found, whereas only background signals were detected on beads incubated with either control Jurkat lysate or no lysate (Fig. 8*C*). In lysates from MFE.htmζ CAR-engrafted Jurkat cells, only a very low level of TCR binding was detected. Mutation of either the disulfide bridge (C2G) or the D6 residue (D6N) of the CAR significantly abrogated coprecipitation of the TCR (Fig. 8*C*). Interestingly, receptor redimerization (C2G G-10C) partially restored TCR interactions, compared with the MFE.C2Gζ receptor. In addition, the MFE.F10Aζ CAR showed TCRβ precipitation capacity equivalent to that of the MFEζ receptor, again suggesting that the effects seen were specific to the particular residues, not simply due to the effect of any mutation in the transmembrane domain (Supplemental Fig. 2*E*). In all cases, there were no significant differences in the amount of CAR bound to the beads (Fig. 8*D* and Supplemental Fig. 2*F*), indicating nearly equivalent levels of CAR loading onto the anti-FLAG beads.

To address the specificity of the FCIP technique, three surface markers highly expressed in Jurkat T cells were chosen as controls (CD28, CD45RA, and CD95). CD28 and CD95 did not demonstrate any significant binding to the MFEζ receptor. Interestingly CD45RA appeared to coprecipitate with MFEζ, an observation that may be related to the role of CD45 as a phosphatase. Interactions between CD3ζ and CD45 have been previously reported (26) and thus support the flexibility of the FCIP approach (Supplemental Fig. 4*A*). Analysis in primary human T cells supports data from Jurkat T cells (Supplemental Fig. 4*B*). Anti-CD3ε Abs were chosen over anti-TCRβ Abs owing to the polyclonality of the populations being investigated. CD3ε was found in association with MFEζ, but not MFE.htmζ.

In an attempt to further elucidate the complex nature of hetero- and homodimeric CAR containing TCR complexes, native gel analysis was performed. Digitonin lysates prepared from nontransduced Jurkat cells or cells expressing the MFEζ.FLAG CAR or homodimeric-forming C2G G-10C.FLAG CAR were separated on native PAGE gels, transferred to polyvinylidene difluoride membranes, and probed with anti-CD3ζ or anti-FLAG Abs. Supplemental Fig. 5 shows that nontransduced cells present a single immunoreactive band at ~720 kDa (see arrow), indicative of the TCR complex (larger immunoreactive band is unresolved sample). A complex of the same molecular size was present in both transduced cell preparations, suggesting that both hetero- and homodimerizing receptors participated in forming fairly equivalent complexes. In each transduced cell lane, there was a clear range of protein complexes with a smaller size of 480 KDa, but there were no apparent differences between either MFEζ.FLAG or C2G G-10C.FLAG, indicating no specific bias of protein complexes that could be attributed to either receptor.

Discussion

CD3ζ has been widely applied in CAR structure as a powerful driver of signal 1 potentially owing to the number of ITAMs contained in the cytoplasmic domain (11, 12). In this study, expression of the MFEζ CAR in Jurkat T cells induced an upregulation of CD3ε that was mediated by the transmembrane domain and led to an increased cytokine response following OKT3 stimulation. Dimerization has been shown to be essential in enabling CD3ζ to interact optimally with the TCR, to allow TCR surface expression (27), and to mediate optimal cellular activation in a model of mast cell degranulation (28). Given the biological effect of the MFEζ CAR upon Jurkat T cell function, understanding the molecular and biochemical interactions of the CAR with the endogenous TCR is likely to be important for the rational design of future CAR receptors.

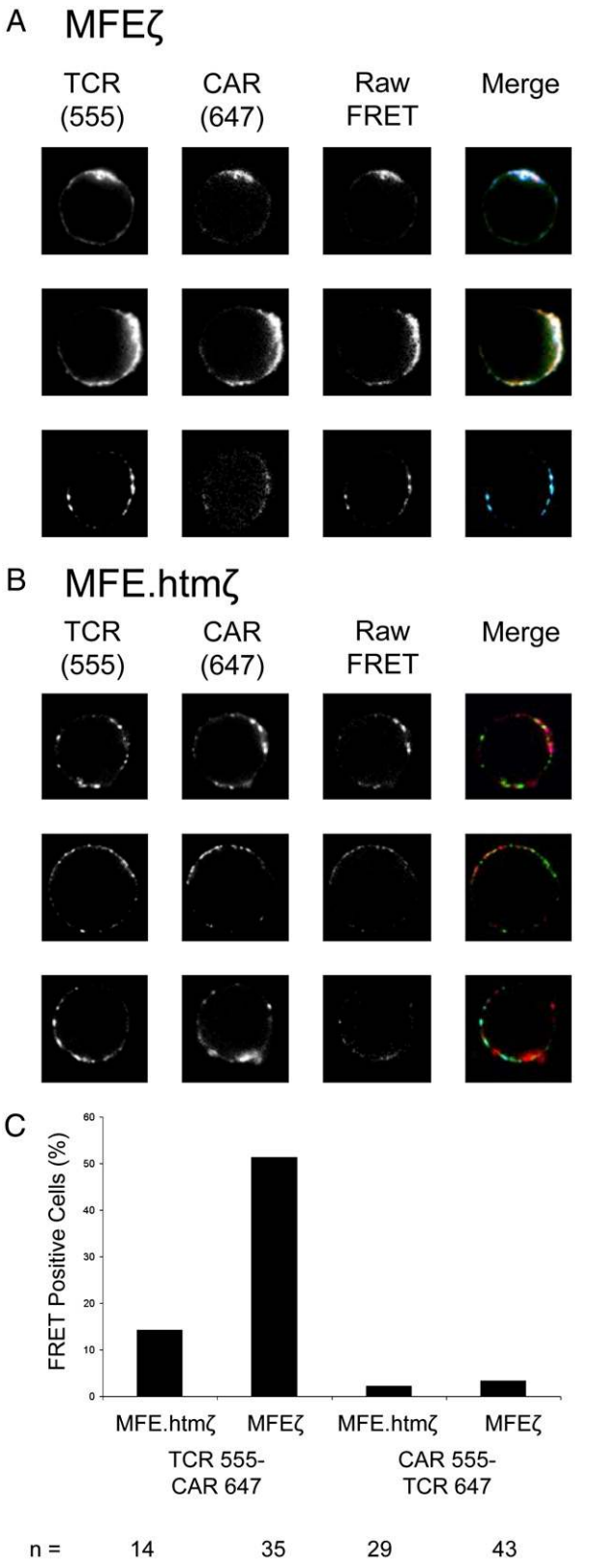

FIGURE 7. FRET analysis of CAR–TCR interactions. Jurkat T cells expressing MFEζ or MFE.htmζ CARs were stained with Alexa Fluor-conjugated anti-TCRVβ8 and truncated CEA protein as indicated, fixed and mounted on slides, and analyzed with an Axiovert time lapse microscope using Metamorph software. Examples of images captured are shown in *A* (MFEζ) and *B* (MFE.htmζ). FRET-positive cells were enumerated for Alexa Fluor 555- and Alexa Fluor 647-conjugated anti-TCRVβ8 and tCEA in both conjugate orientations (*C*). Number of cells analyzed is indicated.

The transmembrane domain of the TCR has previously been identified as an important structural component for transmitting optimal signals to the interior of the cell (28, 29) and in mediating cell surface interactions (21), whereas the transmembrane D6 residue of CD3ζ has been directly implicated in mediating CD3ζ–TCR interactions (18). To determine whether the transmembrane domain of the CAR was driving the functional interaction of this receptor with the endogenous TCR, mutations of amino acid residues thought to be important in protein–protein interactions were generated based upon previous observations. The choice of a C2G mutation to prevent dimerization was based on the work of Bolliger and Johansson (17). Other groups have used C2S (27) mutations to investigate the role of CD3ζ dimerization. Our results demonstrate that a C2G mutation is sufficient to abrogate dimerization of MFEζ, even in the presence of mild detergents such as CHAPS with immunoblotting, indicating that the scFv plays no role in supporting interchain interactions. Immunoblotting also confirmed that MFEζ was capable of forming heterodimers with endogenous CD3ζ, an observation that has been documented previously with receptors containing the CD3ζ transmembrane domain (12, 15, 16) or FcεRIγ transmembrane domains (30, 31). Analysis of CD3ε expression in cells transduced with the dimeric or monomeric forms of the receptors provided supporting evidence that MFE23.CD3ζ dimers are responsible for the observed upregulation of CD3ε.

Interestingly, we have demonstrated that dimerization not only affects CAR–TCR interactions but also has a profound effect on receptor function. This is not the first time that this has been reported (28). However, a previous study used a wild-type CD3ζ molecule harboring a D6A mutation to prevent dimer formation due to rapid internalization of C2A mutants. In this current study, there were no issues concerning expression of the MFEζ C2G mutant, suggesting that the rapid internalization of monomers observed in this report may be related to the cells in which the receptor was expressed. The reason why the C2G mutant was less effective than the MFEζ receptor at inducing T cell activation remains unclear; however, there are several hypotheses. The first possibility is that TCR interactions mediated by the dimeric receptor has beneficial qualities, possibly by leading to phosphorylation of other chains in the TCR complex with which it is in close contact. A second possibility is that stoichiometrically, ligation of one dimer with one CEA molecule leads to phosphorylation of six ITAMs, whereas in the monomeric receptor, three ITAMs would be phosphorylated. A third possibility is that there are intrinsic signaling differences activated by the dimeric and monomeric receptors.

Whatever the cause of the differences, redimerization of the C2G mutant by introducing an alternative cysteine residue into the CAR extracellular domain partially restored optimal function. Although the MFEζ cysteine residue required for interchain dimerization lies within the plasma membrane, it must lie at a biochemically privileged position, as attempts to move this residue deeper into the transmembrane domain failed to induce dimerization. In fact, at transmembrane position 9, not only was dimerization abrogated but also the resulting receptor (C2G L9C) was markedly affected with regard to Ag sensitivity, suggesting this residue plays an important functional role in CD3ζ signaling. Data supporting this theory come from two-dimensional infrared spectroscopic analysis of the CD3ζ transmembrane domain in which a kink in the dimer at position L9 was identified (32, 33). This kink may play a functional role in regulating the structural deformation or twisting/piston-like movement that is predicted to precede TCR signaling events (34–36).

To investigate the signaling capacity of dimeric but TCR non-interacting receptors, mutations at the transmembrane D6 residue, which have been shown in wild-type CD3ζ to permit dimerization

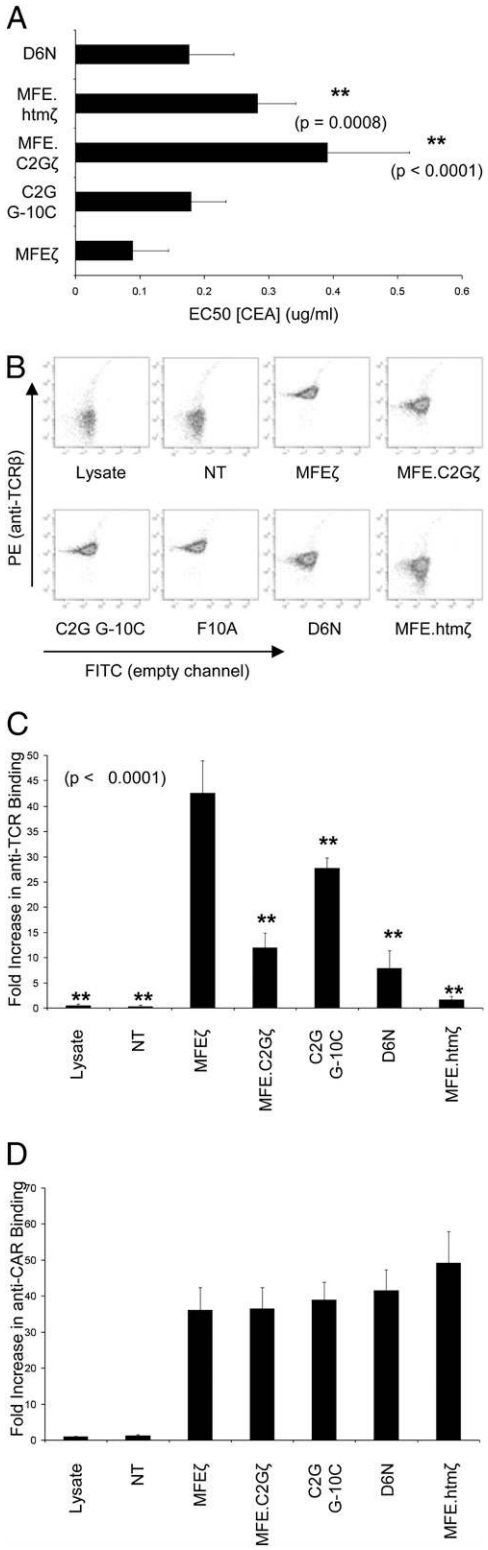

FIGURE 8. FCIP analysis of CAR–TCR interactions in Jurkat T cells. A FLAG tag was cloned onto the C terminus of a panel of existing CARs. The FLAG tag was shown to not affect Ag sensitivity; furthermore, transmembrane mutations affected Ag sensitivity in FLAG-tagged CARs in the same manner as seen with nontagged CARs (*A*). Anti-FLAG–coupled polystyrene beads were incubated with lysates from transduced Jurkat T cells before staining with anti-TCRVβ8 or CEAhFc protein and anti-hIgG. Beads were analyzed using an LSRII cytometer and FlowJo software. Representative scatter plots are shown for anti-TCRVβ8 binding (*B*). Fold increase in Ab binding compared with isotyped control samples was calculated for anti-TCRVβ8 (*C*) or CEAhFc/anti-hIgG (*D*) $**p < 0.01$compared with MFEζ by two-way ANOVA with a post hoc Dunnet test. NT, nontagged.

but abrogate TCR interactions to varying degrees (18, 37), were investigated. The results obtained in this report strongly agree with previous work in wild-type CD3ζ. In particular, an acidic (aspartic acid) to basic (lysine) mutation reduced dimer formation, whereas aspartic acid to asparagine or glutamic acid largely permitted wild-type levels of dimer formation. Rutledge et al. (27) observed that D→K mutations reduced dimer formation by ∼50%, an observation also recorded by Call et al. (18, 21), who showed a reduction in dimer formation even when just one of the aspartic acids in the ζζ pair was mutated to a lysine. The latter reports indicated that glutamic acid and asparagine residues were tolerated more at this position, an observation we have demonstrated in this study of CD3ζ-based CARs. Aspartic acid to glutamine mutations have not previously been tested in wild-type CD3ζ; however, previous analysis in synthetic transmembrane domains revealed that glutamine was capable of mediating oligomerization (38).

Several approaches were used to investigate potential TCR–CAR interactions. In the first instance, we identified an upregulation of CD3ε in Jurkat T cells expressing CAR with the wild-type transmembrane domain. This is an analogous approach to the MA5.8 cells widely used to demonstrate TCR–CD3ζ interactions. The various CARs were expressed in MA5.8 with the finding that any mutation to the transmembrane C2 or D6 residue impacted upon TCR reconstitution. Although the MA5.8 line is murine derived, homology between mouse and human CD3ζ is sufficient to permit interactions to occur. For example, there is just a single amino acid difference (L > I at transmembrane position 16) between the human and mouse CD3ζ transmembrane domain (39). Of interest, a recent publication demonstrated that anything larger than a small epitope tag at the N terminus of CD3ζ abrogated TCR interactions. In this report, CARs containing an α-NIP scFv failed to be incorporated into the TCR complex (40). The conflicting results may be related to the particular scFv used or the level of expression achieved, which was not clearly documented.

The second approach to confirming TCR–CAR interactions was the application of FRET. We chose the best- and worst-performing receptors from the MA5.8 assay with respect to TCR reconstitution. We chose a combination of Alexa Fluor 647 and 555, a combination previously documented to be the optimal FRET pair (41). Of note, it was found that both tCEA and anti-TCRVβ8 had to be conjugated to either and tested in both orientations, as only one orientation demonstrated positive FRET signals. This phenomenon is most likely due to the dependence of positive FRET signals on the donor/acceptor ratio, but only in the case of clustered (e.g., dimeric) but not randomly distributed (e.g., monomeric) molecules (24). This observation therefore implies that, in our model, system surface donor (CAR) is outnumbering the surface acceptor (TCR).

The third approach to defining CAR–TCR interactions was to use a bead-based flow cytometric assay, which enables complexes to be captured on polystyrene beads and then probed for other members of the complex, using flurochrome-conjugated Abs. We have recently reported the development of this technique (25). Using this approach, we have confirmed observations seen in MA5.8 cells. The protein interaction assays raise the question, to what extent are CARs incorporated into TCR? From our current data, it cannot be confirmed whether CAR replaces endogenous CD3ζ in the TCR complex or whether it is incorporated alongside existing molecules. The observation that by FRET large numbers of CARs were often observed in association with TCR suggests that a significant proportion of CAR is interacting with TCR at any one time. This idea is supported by native PAGE analysis, in which we found a considerable amount of the CAR running in the same m.w. range as the endogenous TCR complex.

In this report, mutational, cellular, and biochemical analyses have shown that CD3ζ-based CARs can interact with the TCR complex. Interestingly, this observation contradicts earlier work conducted in scFv.FcεRIγ transduced T cell hybridomas (30), in which CAR expression led to decreased CD3 expression and decreased responsiveness to stimulation. The differences in these results may be attributed to a balance between CAR–TCR interactions and a metabolic load on the transduced cells. In this scenario, non–TCR-interacting CARs would drive down expression of surface receptors owing to the metabolic pressure exerted on the transduced cells. This effect would be partially reversed with TCR-interacting CARs, which would still drive CD3 to the cell surface. Clearly, the interaction of the expressed CAR with endogenous cell surface proteins can have both advantageous and deleterious effects. Understanding the biochemical interactions driven by the CAR receptor will therefore provide important information to aid the future design of this class of proteins.

Acknowledgments

We thank Hayley Batha and Allison O'Neill for helpful technical assistance, Jeff Barry and Michael Hughes (Paterson Institute for Cancer Research Flow Cytometry Group) for invaluable help with flow cytometric sorting of cells, Stuart Pepper and members of the Paterson Institute Molecular Biology Core Facility for sequence analysis, and Prof. David L. Wiest (Fox Chase Cancer Center, Philadelphia, PA) for provision of the MA5.8 cell line. We also thank Prof. Janos Szollosi and Dr. Peter Nagy (University of Debrecen, Debrecen, Hungary) for helpful advice on optimizing FRET analysis, as well as Dr. Reno Debets, Dr. Zsolt Sebestyen, and Coen Govers (Erasmus University, Rotterdam, The Netherlands) for critical analysis of the manuscript.

Disclosures

The authors have no financial conflicts of interest.

References

1. Kershaw, M. H., J. A. Westwood, L. L. Parker, G. Wang, Z. Eshhar, S. A. Mavroukakis, D. E. White, J. R. Wunderlich, S. Canevari, L. Rogers-Freezer, et al. 2006. A phase I study on adoptive immunotherapy using gene-modified T cells for ovarian cancer. *Clin. Cancer Res.* 12: 6106–6115.
2. Park, J. R., D. L. Digiusto, M. Slovak, C. Wright, A. Naranjo, J. Wagner, H. B. Meechoovet, C. Bautista, W. C. Chang, J. R. Ostberg, and M. C. Jensen. 2007. Adoptive transfer of chimeric antigen receptor re-directed cytolytic T lymphocyte clones in patients with neuroblastoma. *Mol. Ther.* 15: 825–833.
3. Schumacher, T. N. 2002. T-cell-receptor gene therapy. *Nat. Rev. Immunol.* 2: 512–519.
4. Morgan, R. A., M. E. Dudley, J. R. Wunderlich, M. S. Hughes, J. C. Yang, R. M. Sherry, R. E. Royal, S. L. Topalian, U. S. Kammula, N. P. Restifo, et al. 2006. Cancer regression in patients after transfer of genetically engineered lymphocytes. *Science* 314: 126–129.
5. Eshhar, Z. 2008. The T-body approach: redirecting T cells with antibody specificity. *Handb. Exp. Pharmacol.* (181):329–342.
6. Garrido, F., F. Ruiz-Cabello, T. Cabrera, J. J. Pérez-Villar, M. López-Botet, M. Duggan-Keen, and P. L. Stern. 1997. Implications for immunosurveillance of altered HLA class I phenotypes in human tumours. *Immunol. Today* 18: 89–95.
7. Restifo, N. P., F. Esquivel, Y. Kawakami, J. W. Yewdell, J. J. Mulé, S. A. Rosenberg, and J. R. Bennink. 1993. Identification of human cancers deficient in antigen processing. *J. Exp. Med.* 177: 265–272.
8. Ferrone, S., and F. M. Marincola. 1995. Loss of HLA class I antigens by melanoma cells: molecular mechanisms, functional significance and clinical relevance. *Immunol. Today* 16: 487–494.
9. Finney, H. M., A. D. Lawson, C. R. Bebbington, and A. N. Weir. 1998. Chimeric receptors providing both primary and costimulatory signaling in T cells from a single gene product. *J. Immunol.* 161: 2791–2797.
10. Finney, H. M., A. N. Akbar, and A. D. Lawson. 2004. Activation of resting human primary T cells with chimeric receptors: costimulation from CD28, inducible costimulator, CD134, and CD137 in series with signals from the TCR zeta chain. *J. Immunol.* 172: 104–113.
11. Haynes, N. M., M. B. Snook, J. A. Trapani, L. Cerruti, S. M. Jane, M. J. Smyth, and P. K. Darcy. 2001. Redirecting mouse CTL against colon carcinoma: superior signaling efficacy of single-chain variable domain chimeras containing TCR-zeta vs Fc epsilon RI-gamma. *J. Immunol.* 166: 182–187.
12. Gilham, D. E., A. O'Neil, C. Hughes, R. D. Guest, N. Kirillova, M. Lehane, and R. E. Hawkins. 2002. Primary polyclonal human T lymphocytes targeted to carcino-embryonic antigens and neural cell adhesion molecule tumor antigens by CD3zeta-based chimeric immune receptors. *J. Immunother.* 25: 139–151.
13. Guest, R. D., R. E. Hawkins, N. Kirillova, E. J. Cheadle, J. Arnold, A. O'Neill, J. Irlam, K. A. Chester, J. T. Kemshead, D. M. Shaw, et al. 2005. The role of extracellular spacer regions in the optimal design of chimeric immune receptors: evaluation of four different scFvs and antigens. *J. Immunother.* 28: 203–211.
14. Finer, M. H., T. J. Dull, L. Qin, D. Farson, and M. R. Roberts. 1994. kat: a high-efficiency retroviral transduction system for primary human T lymphocytes. *Blood* 83: 43–50.
15. Morgenroth, A., M. Cartellieri, M. Schmitz, S. Günes, B. Weigle, M. Bachmann, H. Abken, E. P. Rieber, and A. Temme. 2007. Targeting of tumor cells expressing the prostate stem cell antigen (PSCA) using genetically engineered T-cells. *Prostate* 67: 1121–1131.
16. Sheen, A. J., D. J. Sherlock, J. Irlam, R. E. Hawkins, and D. E. Gilham. 2003. T lymphocytes isolated from patients with advanced colorectal cancer are suitable for gene immunotherapy approaches. *Br. J. Cancer* 88: 1119–1127.
17. Bolliger, L., and B. Johansson. 1999. Identification and functional characterization of the zeta-chain dimerization motif for TCR surface expression. *J. Immunol.* 163: 3867–3876.
18. Call, M. E., J. R. Schnell, C. Xu, R. A. Lutz, J. J. Chou, and K. W. Wucherpfennig. 2006. The structure of the zetazeta transmembrane dimer reveals features essential for its assembly with the T cell receptor. *Cell* 127: 355–368.
19. Zhou, F. X., H. J. Merianos, A. T. Brunger, and D. M. Engelman. 2001. Polar residues drive association of polyleucine transmembrane helices. *Proc. Natl. Acad. Sci. USA* 98: 2250–2255.
20. Blumberg, R. S., B. Alarcon, J. Sancho, F. V. McDermott, P. Lopez, J. Breitmeyer, and C. Terhorst. 1990. Assembly and function of the T cell antigen receptor. Requirement of either the lysine or arginine residues in the transmembrane region of the alpha chain. *J. Biol. Chem.* 265: 14036–14043.
21. Call, M. E., J. Pyrdol, M. Wiedmann, and K. W. Wucherpfennig. 2002. The organizing principle in the formation of the T cell receptor-CD3 complex. *Cell* 111: 967–979.
22. Alarcon, B., B. Berkhout, J. Breitmeyer, and C. Terhorst. 1988. Assembly of the human T cell receptor-CD3 complex takes place in the endoplasmic reticulum and involves intermediary complexes between the CD3-gamma.delta.epsilon core and single T cell receptor alpha or beta chains. *J. Biol. Chem.* 263: 2953–2961.
23. Sussman, J. J., J. S. Bonifacino, J. Lippincott-Schwartz, A. M. Weissman, T. Saito, R. D. Klausner, and J. D. Ashwell. 1988. Failure to synthesize the T cell CD3-zeta chain: structure and function of a partial T cell receptor complex. *Cell* 52: 85–95.
24. Kenworthy, A. K., and M. Edidin. 1998. Distribution of a glycosylphosphatidylinositol-anchored protein at the apical surface of MDCK cells examined at a resolution of <100 A using imaging fluorescence resonance energy transfer. *J. Cell Biol.* 142: 69–84.
25. Bridgeman, J. S., M. Blaylock, R. E. Hawkins, and D. E. Gilham. 2010. Development of a flow cytometric co-immunoprecipitation technique for the study of multiple protein-protein interactions and its application to T-cell receptor analysis. *Cytometry A* 77: 338–346.
26. Furukawa, T., M. Itoh, N. X. Krueger, M. Streuli, and H. Saito. 1994. Specific interaction of the CD45 protein-tyrosine phosphatase with tyrosine-phosphorylated CD3 zeta chain. *Proc. Natl. Acad. Sci. USA* 91: 10928–10932.
27. Rutledge, T., P. Cosson, N. Manolios, J. S. Bonifacino, and R. D. Klausner. 1992. Transmembrane helical interactions: zeta chain dimerization and functional association with the T cell antigen receptor. *EMBO J.* 11: 3245–3254.
28. Gosse, J. A., A. Wagenknecht-Wiesner, D. Holowka, and B. Baird. 2005. Transmembrane sequences are determinants of immunoreceptor signaling. *J. Immunol.* 175: 2123–2131.
29. Yamasaki, S., E. Ishikawa, M. Kohno, and T. Saito. 2004. The quantity and duration of FcRgamma signals determine mast cell degranulation and survival. *Blood* 103: 3093–3101.
30. Annenkov, A. E., S. P. Moyes, Z. Eshhar, R. A. Mageed, and Y. Chernajovsky. 1998. Loss of original antigenic specificity in T cell hybridomas transduced with a chimeric receptor containing single-chain Fv of an anti-collagen antibody and Fc epsilonRI-signaling gamma subunit. *J. Immunol.* 161: 6604–6613.
31. Eshhar, Z., T. Waks, G. Gross, and D. G. Schindler. 1993. Specific activation and targeting of cytotoxic lymphocytes through chimeric single chains consisting of antibody-binding domains and the gamma or zeta subunits of the immunoglobulin and T-cell receptors. *Proc. Natl. Acad. Sci. USA* 90: 720–724.
32. Mukherjee, P., I. Kass, I. T. Arkin, and M. T. Zanni. 2006. Structural disorder of the CD3zeta transmembrane domain studied with 2D IR spectroscopy and molecular dynamics simulations. *J. Phys. Chem. B* 110: 24740–24749.
33. Mukherjee, P., I. Kass, I. T. Arkin, I. Arkin, and M. T. Zanni. 2006. Picosecond dynamics of a membrane protein revealed by 2D IR. *Proc. Natl. Acad. Sci. USA* 103: 3528–3533.
34. Kuhns, M. S., M. M. Davis, and K. C. Garcia. 2006. Deconstructing the form and function of the TCR/CD3 complex. *Immunity* 24: 133–139.
35. Kuhns, M. S., and M. M. Davis. 2007. Disruption of extracellular interactions impairs T cell receptor-CD3 complex stability and signaling. *Immunity* 26: 357–369.
36. Risueño, R. M., W. W. Schamel, and B. Alarcon. 2008. T cell receptor engagement triggers its CD3epsilon and CD3zeta subunits to adopt a compact, locked conformation. *PLoS One* 3: e3911.

37. Call, M. E., J. Pyrdol, and K. W. Wucherpfennig. 2004. Stoichiometry of the T-cell receptor-CD3 complex and key intermediates assembled in the endoplasmic reticulum. *EMBO J.* 23: 2348–2357.
38. Gratkowski, H., J. D. Lear, and W. F. DeGrado. 2001. Polar side chains drive the association of model transmembrane peptides. *Proc. Natl. Acad. Sci. USA* 98: 880–885.
39. Weissman, A. M., D. Hou, D. G. Orloff, W. S. Modi, H. Seuanez, S. J. O'Brien, and R. D. Klausner. 1988. Molecular cloning and chromosomal localization of the human T-cell receptor zeta chain: distinction from the molecular CD3 complex. *Proc. Natl. Acad. Sci. USA* 85: 9709–9713.
40. Minguet, S., M. Swamy, E. P. Dopfer, E. Dengler, B. Alarcón, and W. W. Schamel. 2008. The extracellular part of zeta is buried in the T cell antigen receptor complex. *Immunol. Lett.* 116: 203–210.
41. Horváth, G., M. Petrás, G. Szentesi, A. Fábián, J. W. Park, G. Vereb, and J. Szöllosi. 2005. Selecting the right fluorophores and flow cytometer for fluorescence resonance energy transfer measurements. *Cytometry A* 65: 148–157.